

## Article

# Physiopathological Insights into Atrial Fibrillation Onset through Heart Rate Variability Correlations

Jean-Marie Grégoire <sup>1,2,\*</sup>, Cédric Gilon <sup>2</sup>, François Marelli <sup>3</sup>, Hugues Bersini <sup>2</sup> and Stéphane Carlier <sup>1,4</sup>

<sup>1</sup> Cardiology Department, Université de Mons, 7000 Mons, Belgium; stephane.carlier@umons.ac.be (S.C.)

<sup>2</sup> IRIDIA, Université Libre de Bruxelles, 1050 Bruxelles, Belgium; cedric.gilon@ulb.be (C.G.); hugues.bersini@ulb.be (H.B.)

<sup>3</sup> ISIA Lab, Université de Mons, 7000 Mons, Belgium; francois.marelli@umons.ac.be (F.M.)

<sup>4</sup> CHU Helora, Site Kennedy, 7000 Mons, Belgium

\* Corresponding author. E-mail: jmgregoire3@skynet.be or jean-marie.gregoire@ulb.be (J.-M.G.)

Received: 1 July 2025; Accepted: 27 August 2025; Available online: 29 August 2025

**ABSTRACT:** Atrial fibrillation (AF) is the most common cardiac arrhythmia and is associated with increased morbidity and mortality. Early prediction of AF episodes remains a clinical challenge. This study aimed to generate physiopathological hypotheses for AF onset by analyzing correlations among heart rate variability (HRV) parameters in patients monitored via long-term Holter ECG. We utilized the IRIDIA-AF database, comprising 1319 paroxysmal AF episodes from 872 patients. An XGBoost machine learning model was developed to predict AF onset within 24 h using short- and long-term HRV features, fragmentation indices, and non-linear metrics extracted during sinus rhythm. Model interpretation was performed using SHapley Additive exPlanations (SHAP) values, and dimensionality reduction techniques were applied for data visualization. The model achieved an area under the receiver operating characteristic curve of 0.919 and an area under the precision-recall curve of 0.919, with high accuracy, sensitivity, and specificity. Key predictive features included short-term vagal activity, HRV fragmentation indices, and non-linear parameters, highlighting the role of the autonomic nervous system in AF initiation. Our findings suggest that distinct physiological profiles, detectable via HRV, may underlie AF susceptibility and could inform personalized monitoring and prevention strategies.

**Keywords:** Atrial fibrillation; Machine learning; Onset prediction; Physiopathology; Heart rate variability; Heart rate fragmentation; Non-linearities



© 2025 The authors. This is an open access article under the Creative Commons Attribution 4.0 International License (<https://creativecommons.org/licenses/by/4.0/>).

## 1. Introduction

Atrial fibrillation (AF) is the most common cardiac arrhythmia. Confirmation by an electrocardiogram (12-lead, multiple, or single leads) is recommended to establish the diagnosis of clinical AF. The time period of AF required for diagnosis on monitoring devices is unclear. A standard 12-lead ECG measures 10 s, while 30 s or more on single-lead or multiple-lead ECG devices has generally been the consensus opinion, albeit with limited evidence [1]. More than 80% of patients with ischemic stroke have underlying AF, and the condition doubles the risk of mortality [2]. The incidence of AF is rising over time. The number of affected patients is increasing more rapidly than the general population [3]. According to a recent study, the global incidence of AF in 2019 was approximately 4.72 million new cases per year, and the global prevalence was about 59.70 million cases in the world [4].

Recent advances in machine learning now make it possible to identify patients who are likely to experience AF episodes while still in sinus rhythm, using techniques applied to the ECG signal [5]. This can be achieved either from the raw ECG tracing or heart rate variability (HRV) parameters [6]. While the raw ECG signal itself does not provide insights into the underlying pathophysiology, HRV reflects the activity of the autonomic nervous system (ANS) and thus offers clues about the physiological mechanisms involved [7].

The aim of this study is to analyze the correlations between various HRV parameters in patients who are about to experience an episode of AF within the next 24 h, as identified by Holter ECG monitoring. The goal is to generate hypotheses regarding the factors that trigger AF episodes.

## 2. Materials and Methods

This study builds upon data and findings from a recently published work [6]. We used the IRIDIA-AF database, a curated repository of long-term ECG recordings with expert annotations of paroxysmal AF episodes. The dataset includes 1319 annotated paroxysmal AF episodes from 872 patients. Each recording contains periods of sinus rhythm and one or more episodes of AF. The annotation methodology has been described in detail in the original publication.

For this work, we selected 835 AF episodes of at least 5 min, preceded by at least 60 min of sinus rhythm during the first hour, followed by at least 10 min of sinus rhythm. An XGBoost model was developed to predict the onset of AF episodes within 24 h, using 46 HRV parameters extracted from the first hour of sinus rhythm. The complete list of parameters is provided in the supplementary materials.

To interpret the contribution of each feature to the model's predictions, we used SHapley Additive exPlanations (SHAP) scores [8]. SHAP breaks down the model output into the additive impact of each feature, providing a transparent interpretation of the machine learning model's decision-making process. To uncover redundant information and guide feature reduction, we computed the pairwise Spearman rank-order correlation coefficients among all transformed HRV metrics. This method was selected due to its suitability for capturing non-linear and monotonic relationships frequently observed in HRV data. Before calculating the correlations, all feature values were transformed into their absolute values to minimize the influence of outliers and emphasize the strength of association between variables, regardless of directionality.

Three widely used dimensionality reduction techniques were applied: Principal Component Analysis (PCA), Uniform Manifold Approximation and Projection (UMAP) and t-distributed stochastic neighbor embedding (t\_SNE) [9–11]. Those methods enable the visualization of high-dimensional data in a lower-dimensional space. On the one hand, we used PCA to provide a linear reduction of the dimensionality of the data. On the other hand, we employed UMAP and t-SNE to capture non-linear relationships and uncover more complex hidden structures in the data.

As the HRV must be calculated based on the sinus rhythm, cubic spline interpolation was used in cases of premature atrial complexes (PACs) [12].

## 3. Results

The XGBoost model using the 46 HRV parameters as input features achieved an area under the receiver operating characteristic curve (AUROC) of 0.919 (95% CI: 0.879–0.958) and an area under the precision-recall curve (AUPRC) of 0.919 (95% CI: 0.879–0.958). Using a threshold of 0.5, the model yielded an overall accuracy of 84.5% (95% CI: 81.2–87.8), a sensitivity of 83.0% (95% CI: 79.5–86.4), and a specificity of 86.6% (95% CI: 79.3–93.9). The positive predictive value (PPV) was 90.2% (95% CI: 85.5–94.9), the negative predictive value (NPV) was 78.4% (95% CI: 74.7–82.1), and the F1 score was 86.2% (95% CI: 83.5–89.0) for the entire patient cohort.

According to SHAP value analysis, the most influential features in our XGB model were, in decreasing order of importance: RMSSD (root mean square of successive differences); PAS (percentage of alternating segments); SODP Q1 (number of RR interval differences in the first quadrant of the SODP (second order difference plot)); SODP CTM100 (proportion of SODP points within a circle of radius 100 ms centered at the origin, CTM: central tendency measure); and SD1/SD2, the ratio of SD1 (standard deviation perpendicular to the line of identity) to SD2 (standard deviation along the line of identity) derived from the Poincaré plot (Figures 1 and 2). These were followed by 41 additional dependent variables with progressively lower contributions to the model's predictions.

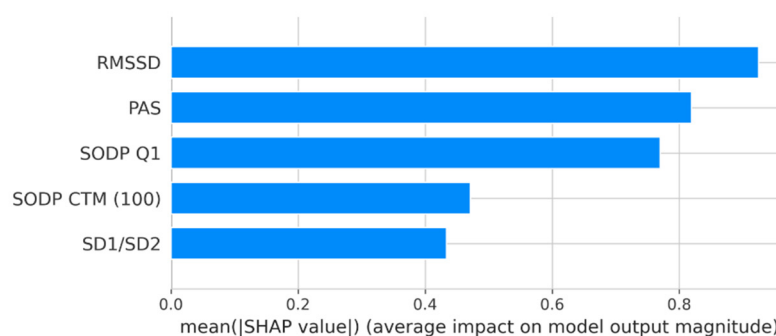


**Figure 1.** SHAP analysis results: top 5 features ranking. RMSSD (root mean square of successive differences); PAS (percentage of alternating segments); SODP Q1 (points in first quadrant of second-order difference plot); SODP CTM100 (points within 100-ms radius circle at origin); SD1/SD2 (Poincaré plot ratio).

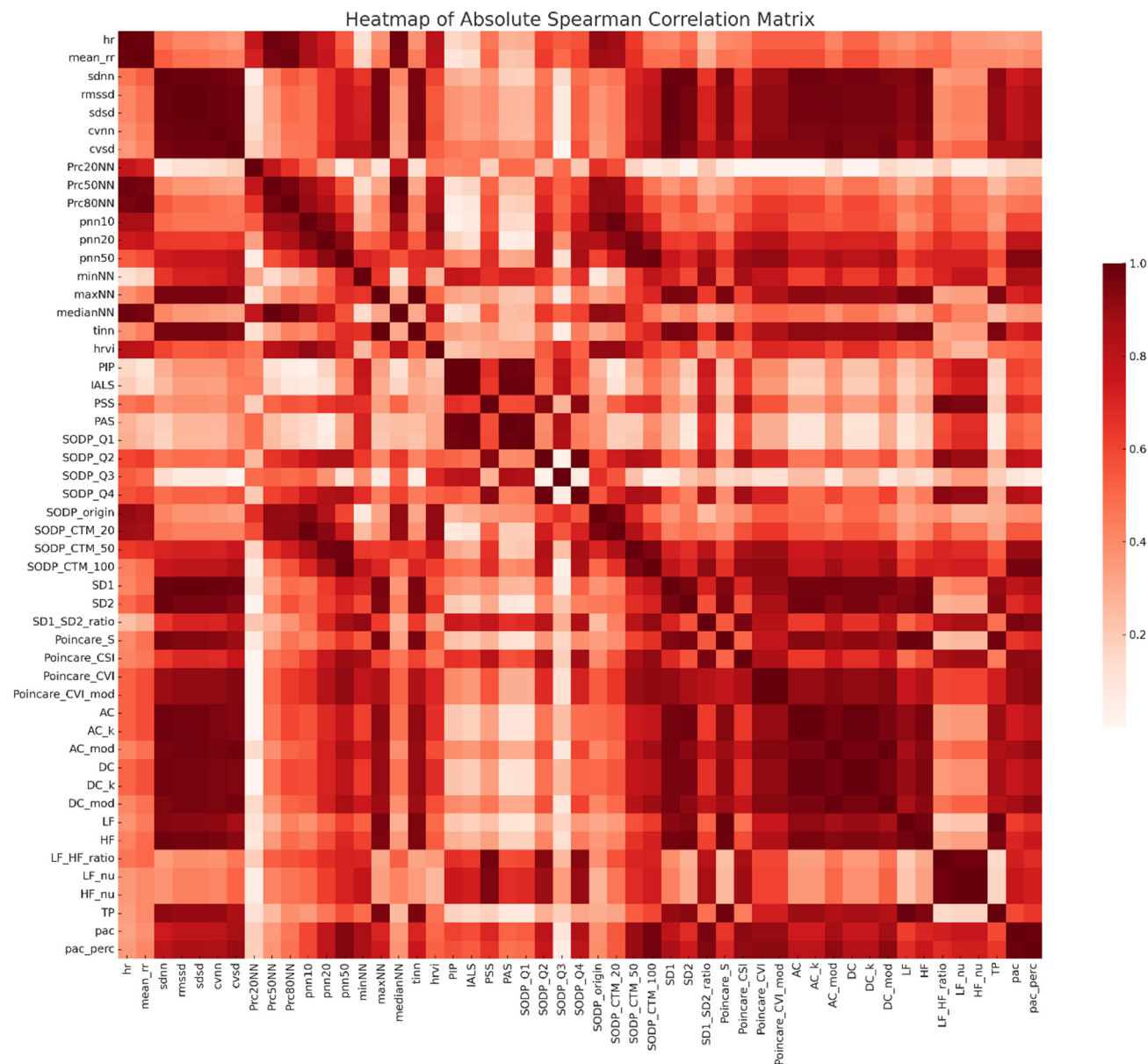


**Figure 2.** Heatmap of the absolute Spearman correlation matrix between heart rate variability (HRV) parameters. This heatmap illustrates the absolute values of Spearman rank correlation coefficients calculated between all pairs of HRV parameters. By taking the absolute values of the correlation coefficients, both positive and negative monotonic associations are treated equally, allowing for a clearer visualization of the overall strength of inter-parameter relationships, irrespective of directionality. The color scale reflects the magnitude of the correlation, with darker shades of red indicating stronger associations. The different 46 HRV parameters are detailed in the supplementary materials.

The 2-dimensional PCA plot presented in Figure 3 shows the distribution of data across the first two principal components, PC1 and PC2. It illustrates a broad spread of data points across both axes.

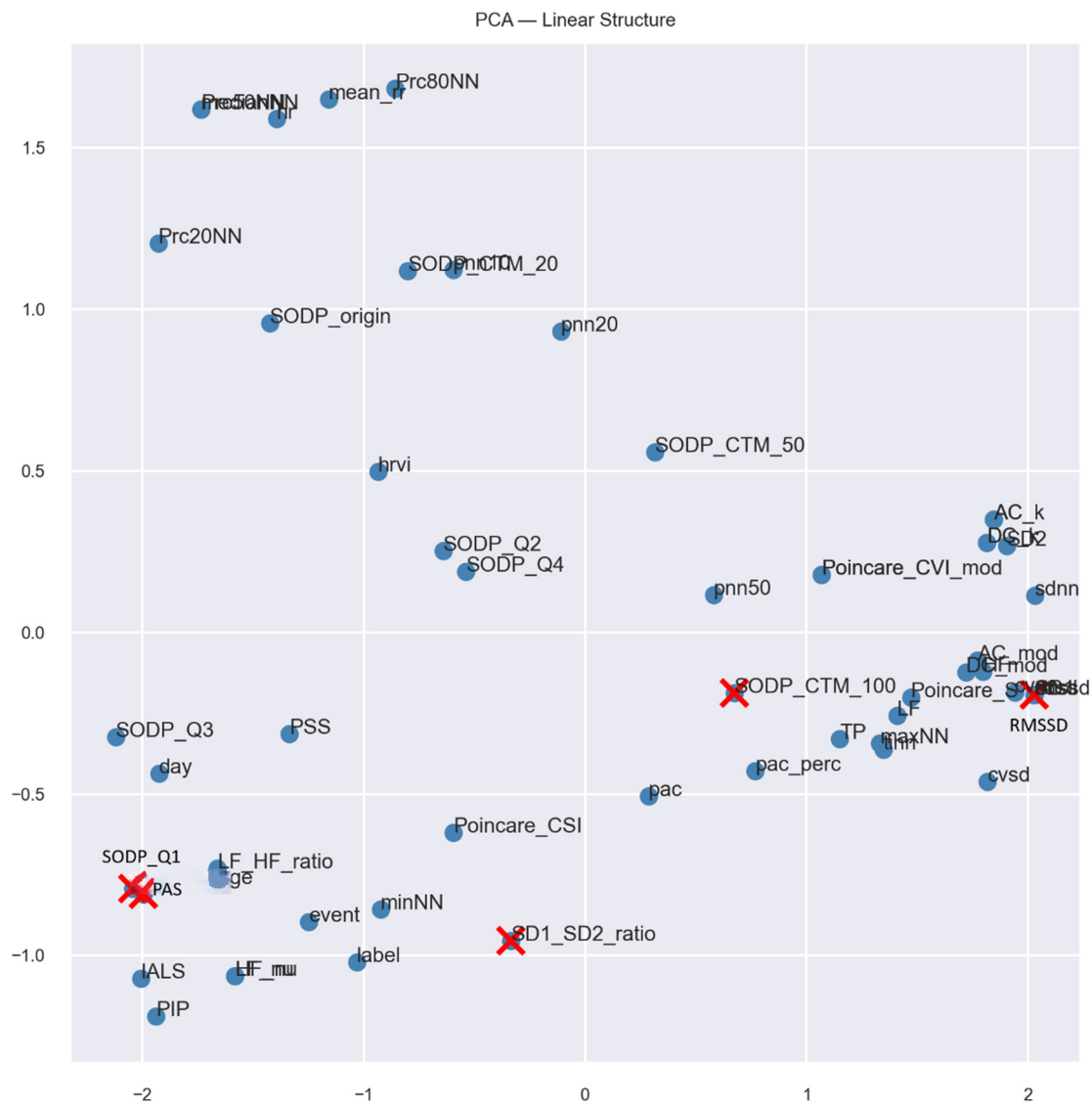


**Figure 3.** Two-dimensional PCA projection of the HRV parameter correlation matrix. Each point represents a feature used in the model, positioned based on its linear relationship with others. The x-axis and y-axis correspond to the first and second principal components (PC1 and PC2), which capture the greatest data variance. Five key features, RMSSD, PAS, SODP\_Q1, SODP\_CTM\_100, and SD1\_SD2\_ratio, are highlighted with red crosses. RMSSD (root mean square of successive differences); PAS (percentage of alternating segments); SODP Q1 (points in first quadrant of second-order difference plot); SODP CTM100 (points within 100-ms radius circle at origin); SD1/SD2 (Poincaré plot ratio).

In contrast, the 2-dimensional UMAP and t\_SNE plots presented in Figures 4 and 5 show a more pronounced structure in the data. We can observe several distinct regions, indicating the presence of groups that are spatially separated within the feature space. It was able to uncover complex relationships that PCA has missed. This separation of data points suggests that HRV features could capture different physiologic profiles, possibly corresponding to different physiologic mechanisms.

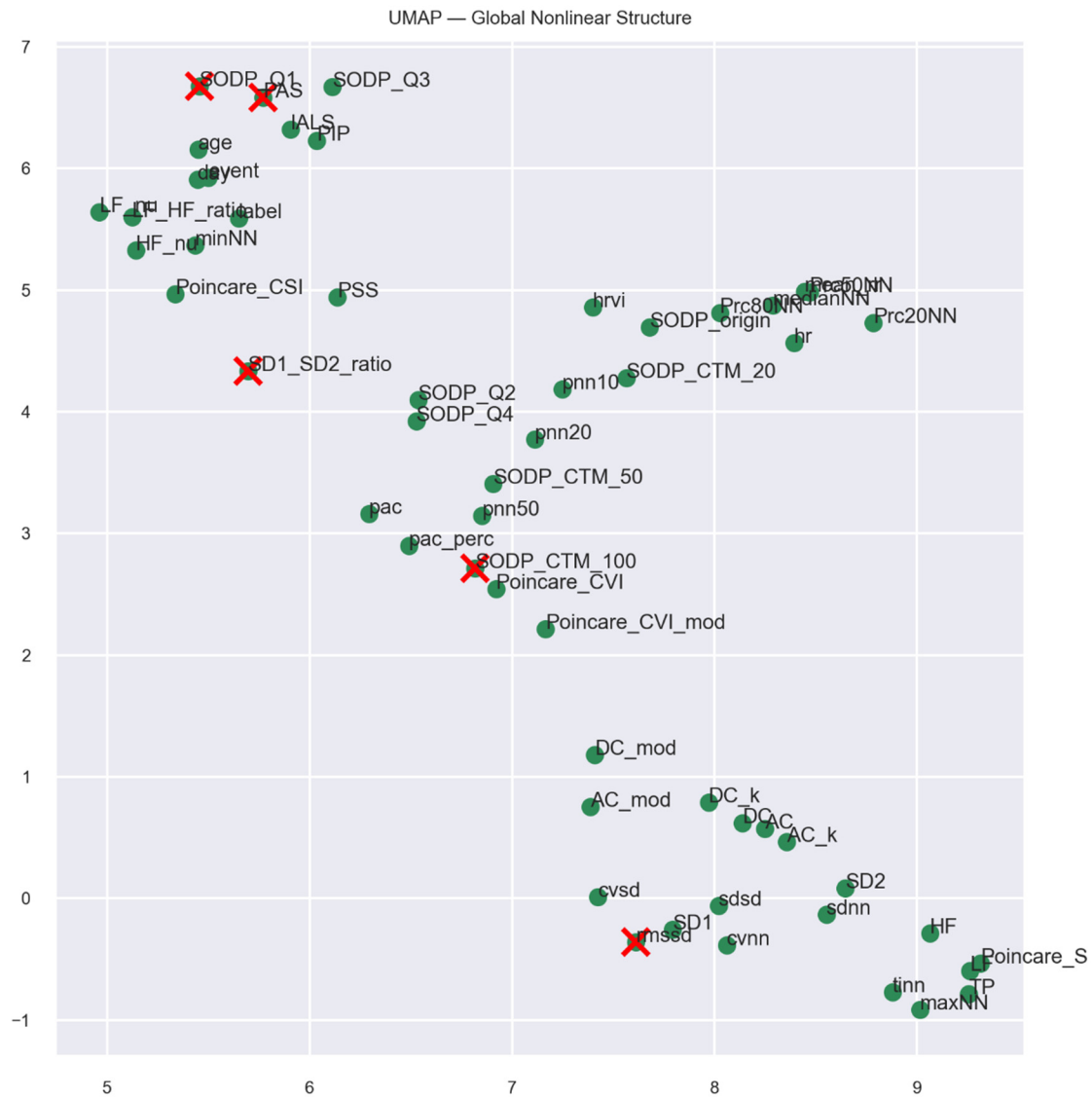


**Figure 4.** Two-dimensional UMAP projection of the HRV feature correlation matrix. Each dot represents a feature, mapped based on its non-linear similarity to others. The  $x$ -axis and  $y$ -axis correspond to the first and second UMAP components, which preserve the global structure of the original high-dimensional data. Key predictors, RMSSD, PAS, SODP\_Q1, SODP\_CTM\_100, and SD1\_SD2\_ratio, are marked with red crosses, RMSSD (root mean square of successive differences); PAS (percentage of alternating segments); SODP Q1 (points in first quadrant of second-order difference plot); SODP CTM100 (points within 100-ms radius circle at origin); SD1/SD2 (Poincaré plot ratio).

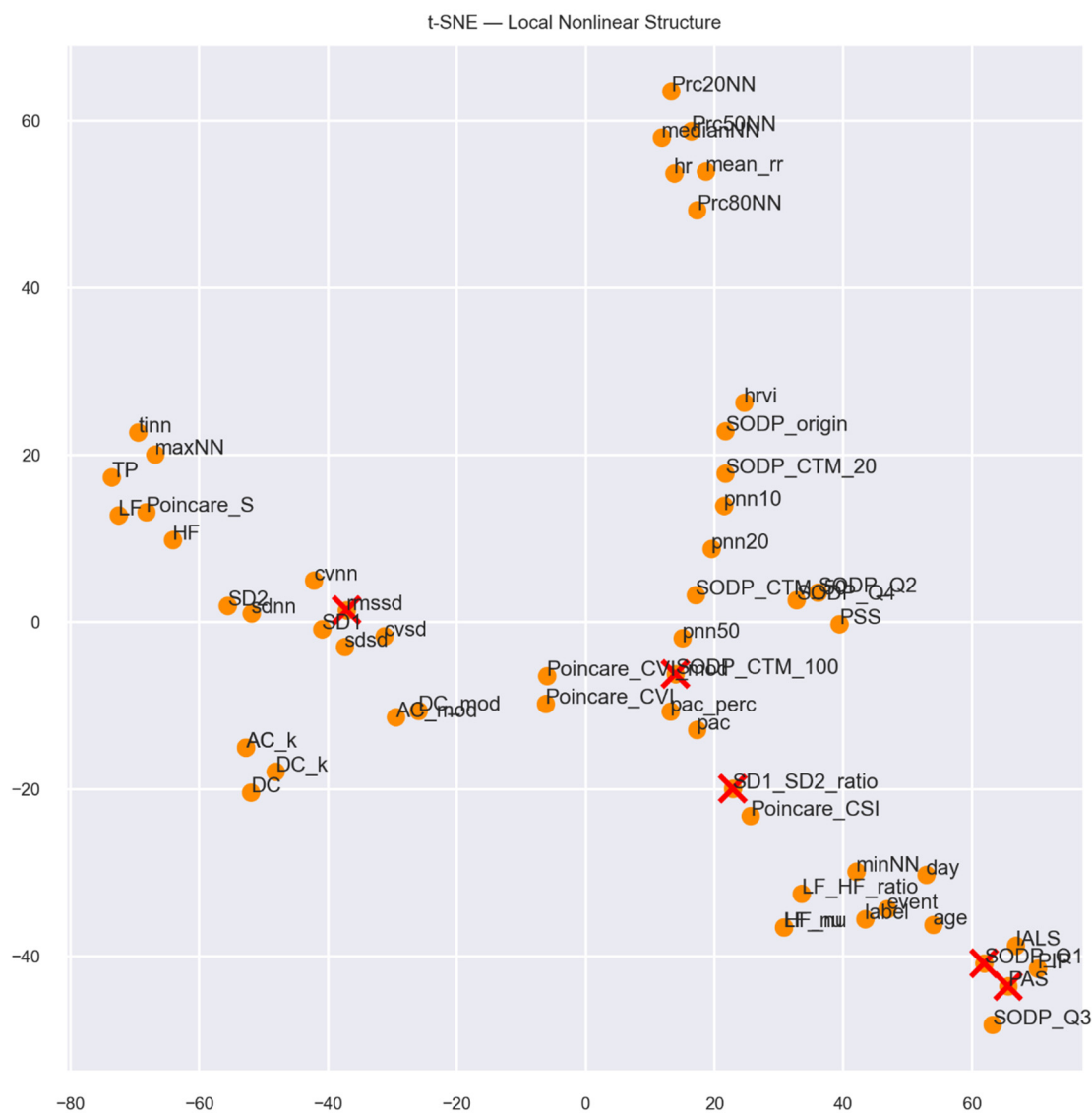


**Figure 5.** Two-dimensional t-SNE projection of the HRV feature correlation matrix. Each point represents a model input feature, positioned based on its local similarity to others. The x-axis and y-axis correspond to the first and second t-SNE components, which preserve the local structure of the high-dimensional space. The five most influential features in the XGB model, RMSSD, PAS, SODP\_Q1, SODP\_CTM\_100, and SD1\_SD2\_ratio, are highlighted with red crosses, as identified by SHAP value analysis RMSSD (root mean square of successive differences); PAS (percentage of alternating segments); SODP Q1 (points in first quadrant of second-order difference plot); SODP CTM100 (points within 100-ms radius circle at origin); SD1/SD2 (Poincaré plot ratio).

#### 4. Discussion

Our study identified five key HRV parameters primarily responsible for the accuracy of short-term prediction of paroxysmal AF episodes. Each parameter reflects a distinct class of pathophysiological mechanisms that trigger such episodes. An important point to note is that PACs are known to trigger AF episodes, their number increases before these episodes, and this has already been used in models to predict AF episodes [6]. In this study, HRV calculations were performed on the first hour of recordings, when the number of PACs is low and, moreover, changes in HRV occur before the increase in PACs. Additionally, HRV calculations were performed using cubic spline interpolation of RR intervals, thereby excluding PACs from the predictions.

As shown in Figure 2, our approach highlights groups of HRV features with closely related variability patterns, enabling clear cluster identification and interpretation across physiological domains (e.g., time-domain, frequency-domain, and non-linear metrics). Using Spearman's method ensures robustness to non-linear relationships and non-normal data distributions, both of which are common in HRV datasets. As illustrated in Figure 3, the HRV feature set exhibits substantial variability. Notably, the five most important predictive parameters are distributed across different regions of the PCA space, indicating minimal redundancy among them.

According to the SHAP scores, the parameters used by the decision tree, in order of importance, are: RMSSD, PAS, SODP\_Q1, SODP\_CTM100, and SD1/SD2. This indicates that the model identified these parameters as the most predictive. The dimensionality reduction analyses (t-SNE, UMAP, PCA) performed on the absolute Spearman correlation matrix revealed consistent and physiologically meaningful clustering patterns among the HRV parameters. Notably, the projections highlighted distinct groupings centered around five key parameters: RMSSD, PAS, SODP\_Q1, SODP\_CTM\_100, and SD1/SD2. These clusters likely reflect different underlying physiological domains contributing to heart rate dynamics.

RMSSD corresponds to the time-domain statistical HRV metrics computed over 5-min segments. It is a well-established marker of short-term vagal activity [13].

PAS is an index belonging to the cluster of fragmentation parameters that capture disruptions in the neuroautonomic-electrophysiological regulation of cardiac rhythm, a phenomenon frequently associated with aging and the progression of cardiovascular disease [14]. Altered PAS values have been linked to ANS dysfunction and may reflect underlying sick sinus syndrome, a condition often implicated in the pathogenesis of atrial fibrillation [15].

SODP\_Q1 corresponds to the first quadrant of the SODP derived from RR interval variations. This quadrant captures sequences in which both the current and previous RR interval differences are positive, reflecting a progressive slowing of the heart rate over three consecutive beats [16]. SODP\_Q1 is thus considered a marker of very short-term vagal modulation [17]. Its relevance in the model underlines the importance of rapid, transient parasympathetic influences detectable at the beat-to-beat level. Interestingly, both PAS and SODP\_Q1 belong to the same cluster in our analysis, suggesting a potential physiological link between neuroautonomic fragmentation and short-term vagal modulation. This association supports the hypothesis that episodes of abrupt changes in cardiac rhythm variability and transient vagal surges may share common pathophysiological substrates in the development of AF.

SODP\_CTM\_100 belongs to the cluster of central tendency measures (CTMs) derived from the SODP, which are designed to quantify the overall degree of variability within the plot. This parameter captures global variability, encompassing short-term, long-term, and non-linear components of the RR interval dynamics [18].

SD1/SD2, the fifth factor corresponds to the balance between short- and long-term variability in RR intervals. Specifically, the width of the Poincaré plot (SD1) reflects the magnitude of short-term heart rate variability (HRV), while its length (SD2) represents long-term variability. The SD1/SD2 ratio, derived from these two measures, captures the relationship between these distinct temporal components of HRV. This parameter appears isolated from the other clusters in our analysis, suggesting that it reflects a distinct, predominantly non-linear aspect of heart rate dynamics [19].

To the best of our knowledge, no prospective or randomized study has yet addressed the short-term prediction of AF onset using HRV or other ECG-derived metrics. Existing work in this field is limited to a few studies that identified an AF “signature” from 12-lead ECGs recorded months before the arrhythmia, which fundamentally differs from our objective of predicting AF onset within a 24-h time window [5,20–22]. Based on two-week Holter monitoring, only one retrospective analysis reported AF prediction several days in advance [23]. Our approach is therefore distinct in targeting an actionable, short-term prediction horizon (<24 h) using Holter-derived HRV features, with the potential to support timely, preventive clinical interventions.

It should be noted that variations in HRV are not specific to the condition under investigation and can be observed in a broad range of clinical contexts. Any disorder affecting the autonomic nervous system has the potential to modify HRV. Cardiac conditions such as acute or chronic heart failure, particularly during decompensation, and coronary artery disease are commonly associated with a global reduction in HRV, reflecting an imbalance with increased sympathetic and reduced parasympathetic activity. Beyond cardiac disorders, several non-cardiac conditions, including diabetes mellitus and other forms of dysautonomia, can also impair autonomic regulation and induce significant alterations in HRV patterns [17].

Apart from providing insight into the underlying pathophysiology, the identification of the five most significant uncorrelated HRV parameters associated with AF onset offers the opportunity to predict paroxysmal AF episodes using models relying solely on these parameters, thereby reducing model complexity while maintaining predictive performance. This enhances their suitability for integration into wearable devices, such as smartwatches. Ultimately, this could enable a ‘pill-in-the-pocket-like’ preventive strategy, distinct from the conventional approach, which involves taking medication after AF onset, whereby the patient would take a class I antiarrhythmic or a beta-blocker *before* the arrhythmia occurs, when the model predicts an autonomic state indicating a high likelihood of imminent AF.



## 5. Conclusions

We hypothesized that a small set of uncorrelated HRV parameters measured during sinus rhythm could capture distinct physiological mechanisms predisposing to AF and enable accurate short-term prediction. Analysis of a large annotated Holter database with an explainable machine learning model confirmed that five key parameters, RMSSD, PAS, SODP Q1, SODP CTM100, and SD1/SD2, were the most predictive, reflecting complementary autonomic and electrophysiological processes. These results offer new insights into the complex autonomic and electrophysiological processes underlying AF development and support the development of simplified, wearable-compatible models for pre-emptive “pill-in-the-pocket-like” preventive strategies.

## Supplementary Materials

The following supporting information can be found at: <https://www.sciepublish.com/article/pii/657>, Table S1. Heart rate variability (HRV) features used in the analysis.

## Acknowledgments

We would like to thank Laurent Groben, Thomas Nguyen, Bernard Deruyter, and Pascal Godart for providing us with some of the Holter recordings.

## Author Contributions

Conceptualization, J.-M.G.; Methodology, J.-M.G., C.G., F.M.; Software C.G., F.M.; Validation, H.B., S.C. Formal Analysis, J.-M.G. investigation, J.-M.G., C.G., F.M.; Writing—Original Draft Preparation, J.-M.G.; Writing—Review & Editing, J.-M.G., C.G., F.M.; Supervision, S.C., H.B.; Project Administration, J.-M.G.; Funding Acquisition, C.G., F.M.

## Ethics Statement

The study was conducted according to the guidelines of the Declaration of Helsinki. Ethical approval for the use of these data was obtained from the relevant committees: protocol P2017/431 (27 October 2017) and CNER protocol 202101/01 (1 January 2021).

## Informed Consent Statement

Patient consent was waived because this is a retrospective study and it was impossible to locate the patients who had benefited from Holter monitoring; furthermore, the data anonymization process means that it is not possible to locate the patients to ask for their consent.

## Data Availability Statement

The first part of the database (IRIDIA v1) can be downloaded from Zenodo: Cédric Gilon, Jean-Marie Grégoire, Marianne Mathieu, Stéphane Carlier, & Hugues Bersini (2023). IRIDIA-AF, a large paroxysmal atrial fibrillation long-term electrocardiogram monitoring database (1.0.1) [Data set]. Zenodo. <https://doi.org/10.5281/zenodo.8405941>.

## Funding

This work was supported by the French Community of Belgium [FRIA funding: FC 038733] and from the European Union’s Horizon 2020 research and innovation programme under the Marie Skłodowska Curie grant agreement No 101034383.

## Declaration of Competing Interest

The authors declare that they have no known competing financial interests or personal relationships that could have appeared to influence the work reported in this paper.



## References

1. Van Gelder IC, Rienstra M, Bunting KV, Casado-Arroyo R, Caso V, Crijns HJ, et al. 2024 ESC Guidelines for the management of atrial fibrillation developed in collaboration with the European Association for Cardio-Thoracic Surgery (EACTS): Developed by the task force for the management of atrial fibrillation of the European Society of Cardiology (ESC), with the special contribution of the European Heart Rhythm Association (EHRA) of the ESC. Endorsed by the European Stroke Organisation (ESO). *Eur. Heart J.* **2024**, *45*, 3314–3414. doi:10.1093/EURHEARTJ/EHAE176.
2. Kalarus Z, Mairesse GH, Sokal A, Boriani G, Średniawa B, Casado-Arroyo R, et al. Searching for atrial fibrillation: looking harder, looking longer, and in increasingly sophisticated ways. An EHRA position paper. *EP Eur.* **2023**, *25*, 185–198. doi:10.1093/europace/euac144.
3. Lane DA, Skjæth F, Lip GY, Larsen TB, Kotecha D. Temporal trends in incidence, prevalence, and mortality of atrial fibrillation in primary care. *J. Am. Heart Assoc.* **2017**, *6*, e005155. doi:10.1161/JAHA.116.005155.
4. Ma Q, Zhu J, Zheng P, Zhang J, Xia X, Zhao Y, et al. Global burden of atrial fibrillation/flutter: Trends from 1990 to 2019 and projections until 2044. *Heliyon* **2024**, *10*, e24052. doi:10.1016/J.HELIYON.2024.E24052.
5. Attia ZI, Noseworthy PA, Lopez-Jimenez F, Asirvatham SJ, Deshmukh AJ, Gersh BJ, et al. An artificial intelligence-enabled ECG algorithm for the identification of patients with atrial fibrillation during sinus rhythm: a retrospective analysis of outcome prediction. *Lancet* **2019**, *394*, 861–867.
6. Gregoire J, Gilon C, Carlier S, Bersini H. Role of the autonomic nervous system and premature atrial contractions in short-term paroxysmal atrial fibrillation forecasting: Insights from machine learning models. *Arch. Cardiovasc. Dis.* **2022**, *115*, 377–387. doi:10.1016/J.ACVD.2022.04.006.
7. Malik M, Bigger JT, Camm AJ, Kleiger RE, Malliani A, Moss AJ, et al. Heart rate variability. Standards of measurement, physiological interpretation, and clinical use. *Eur. Heart J.* **1996**, *17*, 354–381. doi:10.1093/oxfordjournals.eurheartj.a014868.
8. Ariza-Garzón MJ, Arroyo J, Caparrini A, Segovia-Vargas MJ. Explainability of a Machine Learning Granting Scoring Model in Peer-to-Peer Lending. *IEEE Access* **2020**, *8*, 64873–64890. doi:10.1109/ACCESS.2020.2984412.
9. Greenacre M, Groenen PJ, Hastie T, d’Enza AI, Markos A, Tuzhilina E. Principal component analysis. *Nat. Rev. Methods Primers* **2022**, *2*, 100. doi:10.1038/S43586-022-00184-W.
10. McInnes L, Healy J, Melville J. UMAP: Uniform Manifold Approximation and Projection for Dimension Reduction. February 2018. Available online: <https://arxiv.org/pdf/1802.03426> (accessed on 23 June 2025).
11. Maaten LVD, Hinton G. Visualizing Data using t-SNE. *J. Mach. Learn. Res.* **2008**, *9*, 2579–2605.
12. Choi A, Shin H. Quantitative analysis of the effect of an ectopic beat on the heart rate variability in the resting condition. *Front. Physiol.* **2018**, *9*, 922. doi:10.3389/FPHYS.2018.00922/BIBTEX.
13. Shaffer F, Ginsberg JP. An Overview of Heart Rate Variability Metrics and Norms. *Front. Public Health* **2017**, *5*, 258. doi:10.3389/fpubh.2017.00258.
14. Costa MD, Davis RB, Goldberger AL. Heart rate fragmentation: a new approach to the analysis of cardiac interbeat interval dynamics. *Front. Phys.* **2017**, *8*, 255.
15. Costa MD, Redline S, Soliman EZ, Goldberger AL, Heckbert SR, Rey HA. Fragmented sinoatrial dynamics in the prediction of atrial fibrillation: The Multi-Ethnic Study of Atherosclerosis. *Am. J. Physiol. -Heart Circ. Physiol.* **2021**, *320*, H256–H271. doi:10.1152/ajpheart.00421.2020.
16. Babloyantz A, Destexhe A. Is the normal heart a periodic oscillator? *Biol. Cybern.* **1988**, *58*, 203–211. doi:10.1007/BF00364139.
17. Grégoire JM, Gilon C, Carlier S, Bersini H. Autonomic nervous system assessment using heart rate variability. *Acta Cardiol.* **2023**, *78*, 648–662. doi:10.1080/00015385.2023.2177371.
18. Brennan M, Palaniswami M, Kamen P. Do existing measures of Poincaré plot geometry reflect non-linear features of heart rate variability? *IEEE Trans. Biomed. Eng.* **2001**, *48*, 1342–1347. doi:10.1109/10.959330.
19. Deka B, Deka D. Non-linear analysis of heart rate variability signals in meditative state: A review and perspective. *Biomed. Eng. Online* **2023**, *22*, 1–31. doi:10.1186/S12938-023-01100-3/FIGURES/20.
20. Raghunath S, Pfeifer JM, Ulloa-Cerna AE, Nemani A, Carbonati T, Jing L, et al. Deep Neural Networks Can Predict New-Onset Atrial Fibrillation from the 12-Lead ECG and Help Identify Those at Risk of Atrial Fibrillation-Related Stroke. *Circulation* **2021**, *143*, 1287–1298. doi:10.1161/CIRCULATIONAHA.120.047829.
21. Baek YS, Lee SC, Choi W, Kim DH. A new deep learning algorithm of 12-lead electrocardiogram for identifying atrial fibrillation during sinus rhythm. *Sci. Rep.* **2021**, *11*, 12818. doi:10.1038/S41598-021-92172-5.
22. Yuan N, Duffy G, Dhruva SS, Oesterle A, Pellegrini CN, Theurer J, et al. Deep Learning of Electrocardiograms in Sinus Rhythm From US Veterans to Predict Atrial Fibrillation. *JAMA Cardiol.* **2023**, *8*, 1131–1139. doi:10.1001/JAMACARDIO.2023.3701.
23. Singh JP, Fontanarava J, de Massé G, Carbonati T, Li J, Henry C, et al. Short term prediction of Atrial Fibrillation from ambulatory monitoring ECG using a deep neural network. *Eur. Heart J. -Digit. Health* **2022**, *3*, 208–217. doi:10.1093/EHJDH/ZTAC014.